"Solidifying the Scientific Capabilities of Ohmsett-Wave Hydrodynamics"

Michel C. Boufadel, PhD, PE, Xiaolong Geng, PhD, and Roozbeh Golshan, PhD

The New Jersey Institute of Technology
boufadel@gmail.com; (610) 608-2281

Final Report
November 2, 2016

This study was funded by the Bureau of Safety and Environmental Enforcement (BSEE), U.S. Department of the Interior, Washington D.C. under Contract E14PC00036, Project 1045.

Table of Contents

Page #

List of Tables

Page #

List of Figures

Page #

Executive Summary

The project addressed three aspects of the hydrodynamics related to the Ohmsett wavetank. They are: 1) Evaluate the reflection in the wavetank based wave properties that are commonly generated in the Ohmsett tank. 2) Generate breaking wave conditions in the Ohmsett tank that are reproducible and their mixing energy can be quantified, and 3) Design, using Computational Fluid Dynamics, a system to dissipate the wave energy and thus reduce wave reflection.

Regarding the first objective, we used two methods to evaluate the reflection coefficient, and found that, when the "beach" system is operational, the reflection coefficient in the Ohmsett tank varies from 30% for waves whose period is 3.0 seconds (all methods) to 60% for waves whose period is 2.0 s. For the 2.0 second waves, the elaborate methods gave inconsistent results, which is probably due to the fact that the 2.0 s waves were too steep, and thus, the system was too nonlinear. But in all cases, the reflection coefficients values suggest moderate to high reflection in the tank that would "contaminate" the hydrodynamics, as reflection is minimum at sea.

For the second objective, we used the frequency sweep method and generated reproducible breakers. The breaker was generated as follows: A train of short-period waves (T = 1.5 s and *Stroke* = 5 inches=12.5 cm) was first generated for a duration of 6.0 s (i.e., 4 wave cycles). It was followed by a no-action duration of 18.5 s, and then a train of T = 2.0 s (and *Sroke* = 12 inches=30 cm) were generated for a duration of 10.0 s (i.e., 5 wave cycles). The two wave trains met at around 100 m from the wavemaker, where they resulted in a plunging breaker, as shown in Figure 7. The breaker was also uniform across the width of the tank, which is in stark contrast to the artificial breakers obtained currently. Due to the existing reflection in the tank, we could only generate breakers every two minutes, as we had to let wave reflection dissipate before we started the short-wave train.

For the third Objective, we considered a series of twelve screens spaced by 1.0 m (resulting in 12 m from the back wall to the first screen facing the wavemaker). The first six screens (facing the wavemaker) had a porosity of 75% while the second set of six screens had a porosity of approximately 60%. We also considered two situations: One where the screens were submerged by 0.40 m below the MWL and are 0.90 m above it, and another where the screens were completely submerged. We used computational fluid dynamics to simulate the movement of the waves through the screens. The results indicated that the reflection coefficient was less than 10% and 5% for the partially and completely submerged screens, respectively. This would result in a reduced reflection coefficient in comparison with the current "beach" setup (around 30%). Also, the dynamic pressure on the screens was found to be less than 1.0 KPa (around 0.10 m), a relatively small value that would withstood by steel structures holding the screens.

1. Introduction

The goal of this project was to address three aspects of the hydrodynamics related to the Ohmsett wavetank. They are presented herein as three objectives:

a) Evaluate the reflection in the wavetank based wave properties that are commonly generated in the Ohmsett tank.
b) Generate breaking wave conditions in the Ohmsett tank that are reproducible and their mixing energy can be quantified.
c) Design, using Computational Fluid Dynamics, a system to dissipate the wave energy and thus reduce wave reflection.

The report provides first the Background and Methods, and then the Results. The Background section contains the theoretical background on waves, wave reflection, and wave breaking, along with the operational background of the Ohmsett tank. It also includes the detailed tasks that we aimed to address. That same section includes the Methods where the experimental and numerical tools for the investigation are provided. Results are reported in Section 3.0, which is followed by a Discussion Section (Section 4.0). An Appendix is also reported at the end, and it contains results in the form of figures.

2. Background and Methods

The Ohmsett tank is 203 m long, 3.4 m deep (2.4m water depth), and 20 m wide. The tank is equipped with a flap-type wave generator hinged at the bottom of the tank, which can be programmed to produce various types of waves, namely, regular waves of various periods and irregular waves following the JONSWAP spectrum (Hasselmann, Barnett et al. 1973). Table 1 provides the properties of regular waves that could be generated by the Ohmsett wavemaker for the water depth of 2.4 m. The first two columns were provided by the Ohmsett personnel, and they report the stroke (maximum horizontal displacement of the flap at the water level) and the cycles per minute of the wavemaker. The wave period is simply obtained as:

$$T(\text{in seconds}) = \frac{60}{\text{Cycles per minute}} \qquad (1)$$

In Table 1, one notes that as the stroke increases, the wave period increases. This is because the wavemaker cannot produce too large strokes at high CPM (i.e., short periods), due to power limitation resulting from moving a large volume of water (the wedge between the stroke and the hinge at the bottom). In addition, such a high throughput could cause mechanical failure of the wavemaker.

And expression relating the wave length to the wave period is known as the wave-dispersion equation, vis(Dean and Dalrymple 1991):

$$L = \frac{g}{2\pi} T^2 \tanh\left(\frac{2\pi h}{L}\right) \qquad (2)$$

Where g is gravity acceleration (9.81 m^2/s) and "h" is the water depth, equal to 2.4 m for the Ohmsett tank. In deep water (i.e, when water depth is larger than half of the wave length), Eq. 2 could be simplified to:

$$L(\text{in meter}) = \frac{g}{2\pi} T^2 \cong 1.56\, T^2 \qquad (3)$$

Where T is used in seconds. Using Eq. 3 for a wave period of T=2.0s, the wave length is $L \cong 6.28$ m (Table 1). When the wave period increases, the wave length increases proportionally to the square of the period, and eventually the wave starts "feeling" the bottom. In that case, one needs to use Eq. 2, as done for the wave length in Table 1.

Note that the wave length obtained by Eq. 2 (and Eq. 3) is based on the first-order (linear) theory of waves, which is the same for the second-order (Stokes) theory of waves. Only in the third-order theory (and above) that the wave-dispersion equation becomes different. But the third order theory is too complicated to use for investigation of waves in wavetanks.

The wave height in Table 1 was calculated based on the linear theory of a flap-type wavemaker (Hughes 2005), and the equation is:

$$\frac{H}{S} = \frac{4\sinh(kh)}{\sinh(2kh) + 2kh}\left[\sinh(kh) + \frac{1-\cosh(kh)}{kh}\right] \qquad (4)$$

Where "h" is the water depth, and k is known as the wave number and is given by $k = 2\pi / L$. One notes in Table 1 that the wave height increases gradually until T=2 to 3 seconds, and then starts decreasing, because the stroke of the wavemaker is limited.

Table 1: Properties of waves generated by the wavemaker at Ohmsett. The first two columns were provided by the Ohmsett staff. The wave period is obtained by simply converting from cycles per minute. The wave length was obtained by Eq. 2. The wave height was obtained based on Eq. 4. All equations were based on the linear theory of a waves (Dean and Dalrymple 1991).

Stroke, S (m), Input	Cycles per minute, Input	Wave Period, T, (s), conversion from Column (2)	Wave Length, L (m), Eq. 2	Wave Height, H (m) (Eq. 4)
0.15	45	1.33	2.79	0.25
0.20	40	1.50	3.51	0.31
0.25	40	1.50	3.51	0.38
0.30	40	1.50	3.51	0.46
0.35	35	1.71	4.57	0.49
0.41	35	1.71	4.57	0.56
0.46	30	2.00	6.28	0.54
0.51	30	2.00	6.28	0.6
0.56	30	2.00	6.28	0.66
0.61	30	2.00	6.28	0.72
0.66	25	2.40	9.00	0.6
0.71	25	2.40	9.00	0.65
0.76	25	2.40	9.00	0.69
0.81	20	3.00	14.09	0.47

0.86	20	3.00	14.09	0.5
0.91	20	3.00	14.09	0.53
0.96	15	4.00	25.13	0.29
1.02	15	4.00	25.13	0.31
1.06	12	5.00	39.16	0.22
1.12	12	5.00	39.16	0.24

The wave height, H, of Table 1 is based on Eq. 4, which is plotted in Figure 1 for select strokes. Generated waves cannot have wave heights larger than the theoretical maximum value, as obtained by Stokes some 130 years ago. That maximum is 14% of the wave length viz:

$$H_{\max}(m) = 0.14L = 0.14\frac{g}{2\pi}T^2 \cong 0.22T^2 \qquad (5)$$

Eq. 5 is also plotted in Figure 1, and it shows that a wave height of 0.72 m for T=2.0 s (Table 1) is near the maximum value that could be achieved for that wave period.

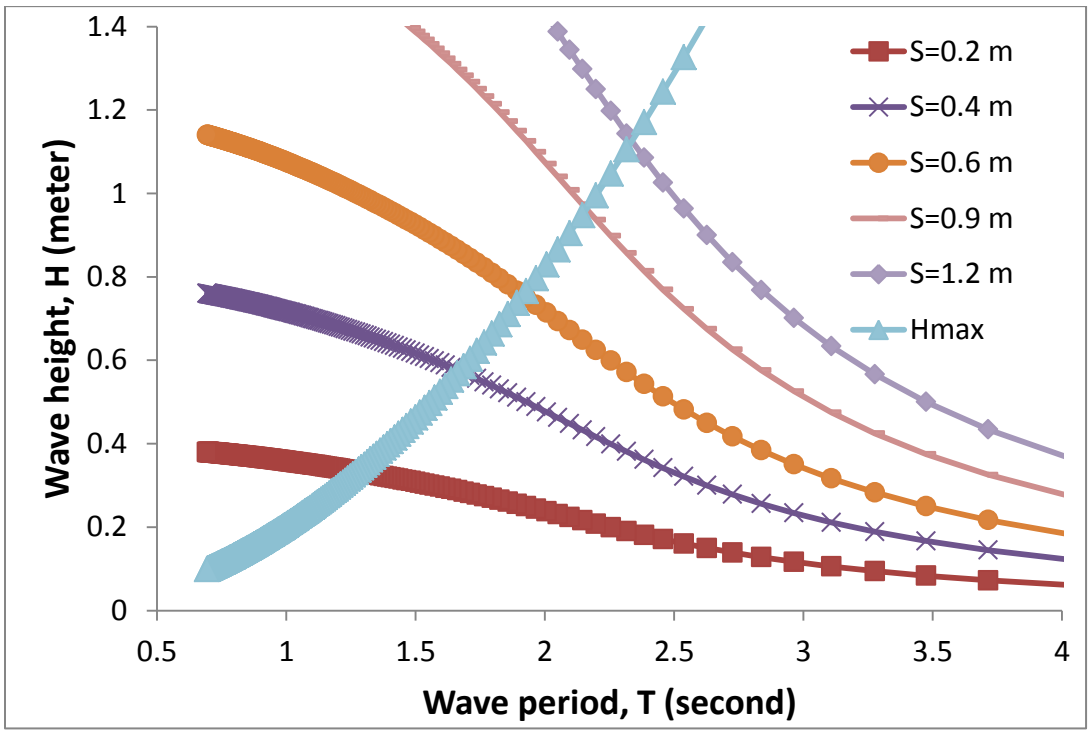

Figure 1: Predicted wave height based on the water depth in the tank (2.4 m) and the stroke of the wavemaker (maximum horizontal displacement of the flap at the water surface) as function of the wave period. Also shown is the maximum theoretical wave height, H_{max}, which is 14% of the wave length.

At the opposite end of the wavemaker, a wave-damping artificial beach made of steel is placed to reduce reflection from the incoming waves. The tank is also equipped with three movable

bridges (i.e., main towing bridge, vacuum bridge, and auxiliary bridge) that span the width of the tank for mounting instruments (e.g., altimeter and high resolution camera).

In this project, the water level due to waves in the tank was measured using four acoustic altimeters of the type Model 300 Sonic Water Level Meter. They were placed as seen in Figure 2a and Figure 2b, and logged to a computer at the Ohmsett. The water velocity in the tank was measured using four Nortek acoustic Doppler velocimeters (ADV) that read at 50 Hz. The ADVs were placed on metallic frames constructed by the NJIT personnel with the support of Ohmsett personnel (Figure 2c). The ADVs produce reliable results when their Signal to Noise Ratio (SNR) is larger than 15 dB (Figure A4) or when the correlation function is larger than 60% (Figure A5).

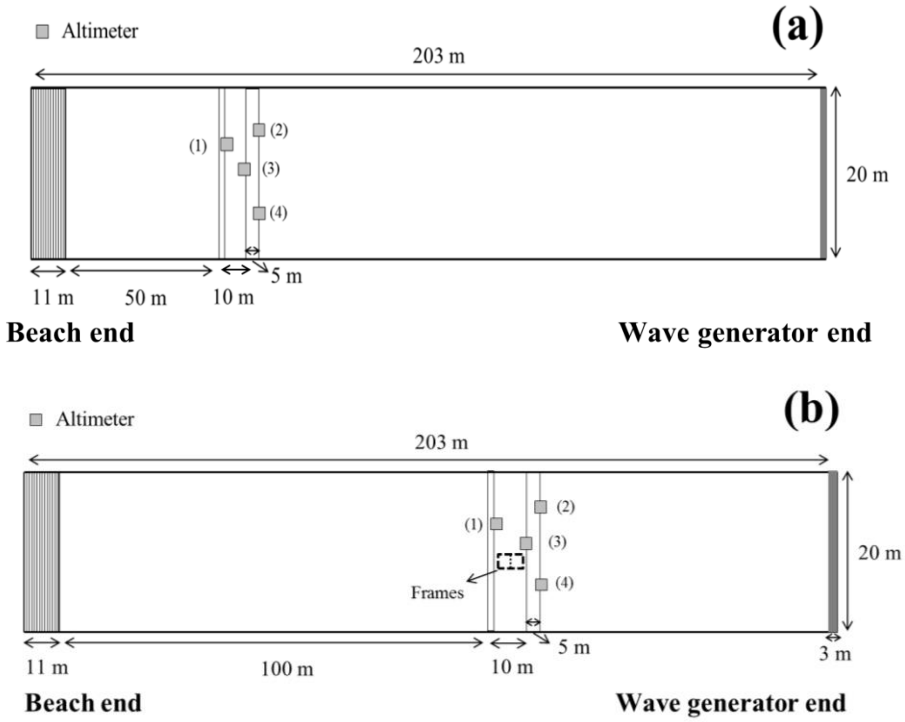

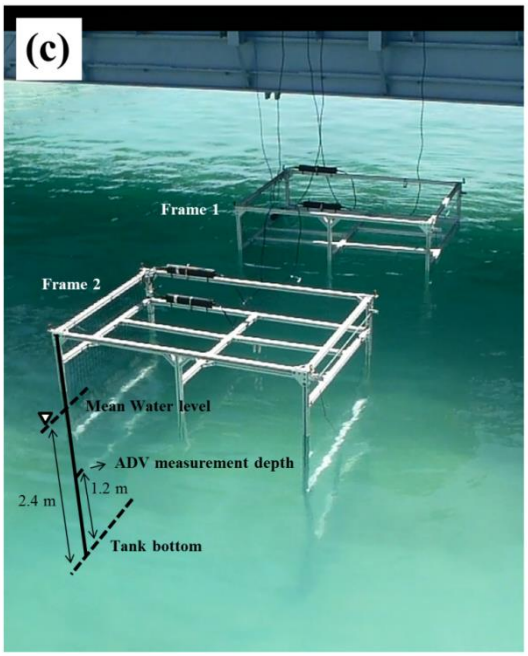

Figure 2: Position of the bridges and altimeters (numbered 1 through 4) in (a) for wave reflection test and in (b) for wave-breaking test. Altimeter 1 was placed on the beach side bridge while altimeters 2, 3, and 4 were placed on the wavemaker side bridge. On that bridge, altimeter 3 was placed on the beach end. (c) frames placed in water and holding the acoustic dopler velocimeters (ADV), at 1.2 m elevation from the bottom. The distance between the exterior of bridges was 10.0 m.

2.1 Wave Reflection

Waves offshore propagate in swells and thus predominantly in one direction for extended durations. The reflected waves from shorelines are damped with distance from the shoreline, and thus become negligible offshore. Therefore, for a wavetank to reproduce offshore wave conditions, its reflected waves would need to be too small to affect wave hydrodynamics. Unfortunately, the existing beach in the Ohmsett still allows for considerable reflection as noted visually; wave generated by the wavemaker operated at a given frequency (e.g., 30 cycles per minute) are initially smooth until they get reflected from the beach side causing the formation of breaking waves in the tank that propagate upstream (i.e., towards the wavemaker), see Figure 3. In fact, the Ohmsett personnel astutely use this fact to conduct dispersion effectiveness testing.

Figure 3: Propagation of the waves and formation of white caps due to reflection from the beach. Normal waves at sea do not break up due to reflection from the beach.

The reflection in a wavetank is evaluated using the Reflection Coefficient R, which is the ratio of the height of the reflected wave H_r to the height of the incident wave H_i (wave height is the vertical distance between the trough and the crest):

$$R = \frac{H_r}{H_i} \tag{6}$$

Thus, if H_r=0, R would be equal to zero, and there would be no reflection, which is the desired situation for a wavetank. If H_R=H_i, then R=1, and 100% of the incident wave would be reflected. Note that the two values H_R and H_i would be embedded within the water profile, and thus would need to be "separate" it mathematically as discussed next.

There are numerous techniques to obtain the reflection coefficient (Dean and Dalrymple 1991, Isaacson 1991). We will consider herein a simple method and two more elaborate methods. The simple method, labeled Method 1 herein, consists of computing the wave height by computing the vertical distance between consecutive crest and troughs based on the water profile, note Figures 6 and 7, discussed later. Then, one locates the maximum and minimum values, H_{max} and H_{min}, respectively, as shown in Figures 6 and 7. The reflection coefficient R is then computed from:

$$R = \frac{H_{max} - H_{min}}{H_{max} + H_{min}} \tag{7}$$

Eq. 7 is an empirical approach to approximate the theoretical value given by Eq. 6. Elaborate methods for computing the reflection coefficient rely on extracting the theoretical values H_i and H_r (i.e., not H_{max} and H_{min}) using three wave gauges (Isaacson 1991), as explained next.

The free surface elevation for normal reflection of regular waves could be assumed to correspond to the superposition of sinusoidal incident and reflected wave trains, and expressed as follows:

$$\eta = \frac{H_i}{2}\cos(kx - \omega t) + \frac{H_r}{2}\cos(-kx - \omega t + \beta) \tag{8}$$

where β denotes a phase angle (in radian) that describes the phase difference between the incident and reflected wave trains at $x = 0$ and $t = 0$; k (radian/m) and ω (radian/s) denote the wave number and wave angular frequency, respectively.

$$\omega = \sqrt{gk \tanh(kd)}, \tag{9}$$

where d denotes the still water depth (2.4 m herein).

The method, labeled Method 2 herein, involves measurements from three probes fixed along wave propagation direction with a distance of λ_2 between altimeters 1 and 2 and λ_3 between altimeters 2 and 3.

In Method 2a, one uses only the average wave height at the three wave gauges (or altimeters): H_1, H_2, and H_3. First defines two quantities A and G:

$$A = \frac{H_i^2 + H_r^2}{4} \tag{10a}$$

$$G = \frac{H_i H_r}{2} \tag{10b}$$

Thus, A is the sum of square of the incident and reflected waves divided by four, and G represents the product of these waves divided by two. From the method, one finds the values of A and G based on the data as:

$$A = \frac{1}{4} \frac{H_1^{\,2} \sin[2k(\lambda_3 - \lambda_2)] - H_2^{\,2} \sin(2k\lambda_3) + H_3^{\,2} \sin(2k\lambda_2)}{\sin[2(k\lambda_3 - k\lambda_2)] + \sin(2k\lambda_2) - \sin(2k\lambda_3)}, \tag{11a}$$

$$G = \frac{1}{8} \{ [\frac{H_1^{\,2} + H_3^{\,2} - 2A}{\cos(k\lambda_3)}]^2 + [\frac{H_1^{\,2} - H_3^{\,2}}{\sin(k\lambda_3)}]^2 \}^{1/2}, \tag{11b}$$

To find the values of the incident and reflected wave heights, one solves Eqs. 10 to obtain:

$$H_i = (\sqrt{A+G} + \sqrt{A-G}), \tag{12a}$$

$$H_r = (\sqrt{A+G} - \sqrt{A-G}), \tag{12b}$$

In a variant of Method 2, Method 2b, the probe signals provide two additional quantities, the phase angle between altimeters 1 and 2, labeled δ_1, and the phase angle between altimeters 1 and 3, labeled δ_2. Then, as the system becomes over-determined (five values at three locations), the five values are obtained by the least square method based on the time series of water levels. The wave heights of the incident and reflected wave trains can be then expressed as:

$$H_i = 2.\left|\frac{s_2 s_3 - 3s_4}{s_5}\right|, \tag{12a}$$

$$H_r = 2.\left|\frac{s_1 s_4 - 3s_3}{s_5}\right|, \tag{12b}$$

Where the quantities "s" are given by:

$$s_1 = \sum_{n=2}^{3} \exp(\mathrm{i}\, 2k\lambda_{\mathrm{n}}), \tag{13a}$$

$$s_2 = \sum_{n=2}^{3} \exp(-\mathrm{i}\, 2k\lambda_{\mathrm{n}}), \tag{13b}$$

$$s_3 = \frac{1}{2}\sum_{n=2}^{3} H_{\mathrm{n}} \exp[\mathrm{i}(\delta_{n-1} + k\lambda_{\mathrm{n}})] \tag{13c}$$

$$s_4 = \frac{1}{2}\sum_{n=2}^{3} H_{\mathrm{n}} \exp[\mathrm{i}(\delta_{n-1} - k\lambda_{\mathrm{n}})] \tag{13d}$$

$$s_5 = s_1 s_2 - 9 \tag{13e}$$

Where "i" is the imaginary unit number (0,-1). The quantities s_1 and s_2 represent thus sums of cosines and sine functions that depend on the wave length. The quantities s_3 and s_4 represent wave heights weighed by the phase angle between the altimeters, and s_5 is simply the product of s_1 by s_2 subtracted by 9.

2.2 Systems to reduce reflection

The dissipation of waves could be conducted using a dynamic or a static system. The dynamic system would be essentially a flap, similar to the one used in the current wavemaker, that would move in response to the incoming water movement such that the reflection is minimized. It is the equivalent of "rolling with the punches". However, the system would be very elaborate, and the flap would not be able to remove simultaneously all the frequencies. For this reason, a static system to dissipate energy is preferred for the Ohmsett tank. The most common choice (Ouellet and Datta 1986) would be a beach system at a mild slope (e.g., 10%) where the water is allowed to run up to lose its kinetic energy and then runs back. But a beach with such a slope might extend too far into the tank. For example, as the water depth is 2.4 m, a beach slope of 10% would extend the beach 24 m into the wavetank, one eighth of the 200 m long tank. In addition, a beach this large might not be easy to remove if one desired various wave configurations in the tank, namely, "harbor chop", which is used in some testing.

An alternative way for dissipating wave energy would be through the usage of a series of porous screens that would be placed vertically at the end opposite the wavemaker (Goda and Ippen 1963, Keulegan 1972, Wickley-Olsen, Boufadel et al. 2007). The latter work was conducted by us the Canada's Department of Fisheries and Oceans (DFO) wavetank in Halifax, Nova Scotia.

An illustration of our proposed idea is shown in Fig. 4 and the goal would be to have each screen lowered into the tank based on need.

There are two important parameters to consider for the design of the screens. They are the porosity and the spacing of the screens. The porosity is defined as:

$$\phi = \frac{\text{Area of opening}}{\text{Area of screen}} \tag{14}$$

Going downstream (i.e., toward the beach), the porosity of each grid and its size of openings should decrease (Le Mehaute 1972). Goda and Ippen (1963) used porosities of 0.30 to 0.50, while Keulegan (1972) used porosities up to 96% (made of fibers). For this reason, we aimed for porosities in the mid-range, (i.e., 60% to 75%), as shown later.

There is no theoretical value for the spacing between the screens or conversely their number. But Goda and Ippen (1963) suggested that the number of screens should be "fairly large". They also proposed that the distance between the first screen and the back wall should be at least equal to one wave length. In our prior work (Wickley-Olsen, Boufadel et al. 2007, Wickley-Olsen, Boufadel et al. 2008), we used 12 screens over 4.0 meters, which was more than double the length of the most frequent wave used in that tank, which was T=1.0 s, giving a wave length L~1.5 m (Eq. 2). And the reflection was below 5% in the DFO tank. The most common wave in the Ohmsett tank has a period of 2.0 s and thus a wave length of approximately 6.0 m.

Based on the literature, our experience, and the properties of the waves in the Ohmsett tank, we selected 12 screens spaced by 1.0 m and the back wall, assuming that the beach is removed from the Ohmsett tank.

2.3 Numerical simulations

A first step in designing the new energy dissipator (or beach) system is to conduct a numerical investigation to simulate the propagation of waves through the screens, to evaluate the reflection coefficient. This approach is essentially a pre-design of the energy dissipator. We used for this purpose the computational fluid dynamics (CFD) software Fluent (www.ansys.com) that we used in prior works (Boufadel, Wickley-Olsen et al. 2008). The goal of the design is to find the configuration of screens that would provide the lowest reflection coefficient (Eq. 6), based on Method 2a (see Methods). The screens could be made of expanded steel sheets (see Figure A6)

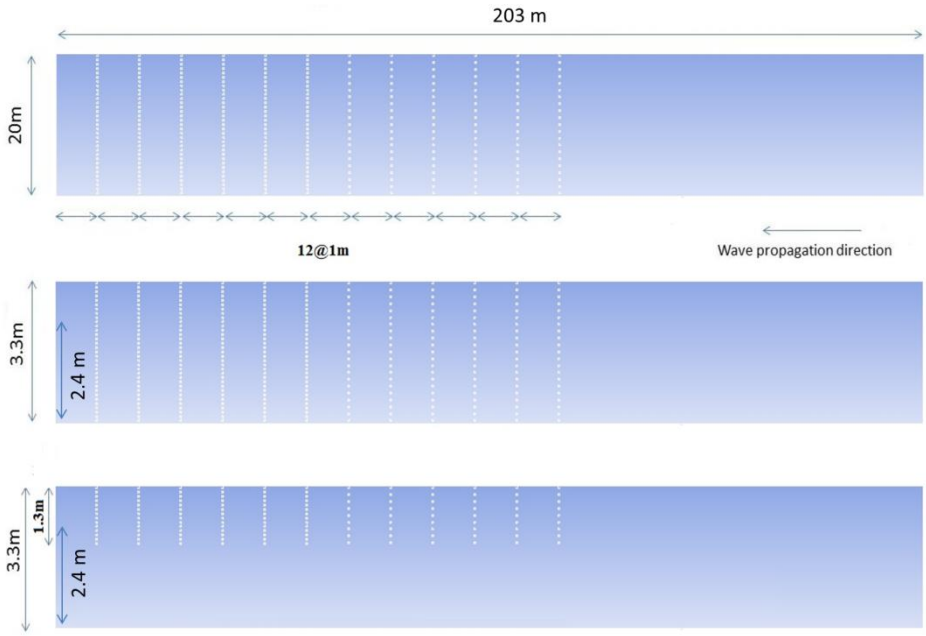

Figure 4: Proposed layout of screens in the Ohmsett tank (after removal of the current beach). The top panel provides a plan view (or top view), the middle panel shows a profile along the wave direction for the fully submerged screens case, and the bottom panel shows a profile along the wave direction of the partially submerged screens case.

Two types of screen submergences were considered, partial and complete. For partial submergence, the screens were assumed submerged to a depth of 0.4 m below the mean water level (MWL), which is at 2.4 m. This leaves 0.90 m of screens above the MWL. In the complete submergence case, the height of the screens was assumed equal to 3.3 m. Thus, the screens would not reach exactly the top of the tank (the concrete wall of the tank), but remain 0.10 m below the top of the tank. Screens at the level of the top of the tank could be a tripping hazard.

For both submergence cases, two sets of screens were considered. The first six screens (i.e., first encountered by the incident waves, Figure 4) had a porosity of ϕ=0.75 (Eq. 14), and the expanded steel rectangular steel cells had an opening of 12 cm. The vertical steel between openings is 4 cm. The second set of six screens had a porosity ϕ=0.60, and the opening of 6.0 cm and the vertical steel width between openings was 4 cm. While the small porosity screens were intended to dissipate the incident waves, the larger porosity screens were selected to dissipate the reflected wave, and this approach is based on our experience with the Bedford Institute of Oceanography wave tank. These porosities can be found in expanded steel screens (Figure A6).

A two-dimensional (vertical) mesh consisting of 869,976 quadrilateral unstructured elements was used for the case with partially submerged screens, and a mesh consisting of 1,200,527 elements was used for the case with fully submerged screen. The mesh size varied from a minimum value of 6 mm near the screens to a maximum value of 30 mm at 0.20 m from the screens for both cases, as illustrated in Figure 5. The time step was 1/10,000 second for both cases, and an implicit second-order scheme was used to integrate over time.

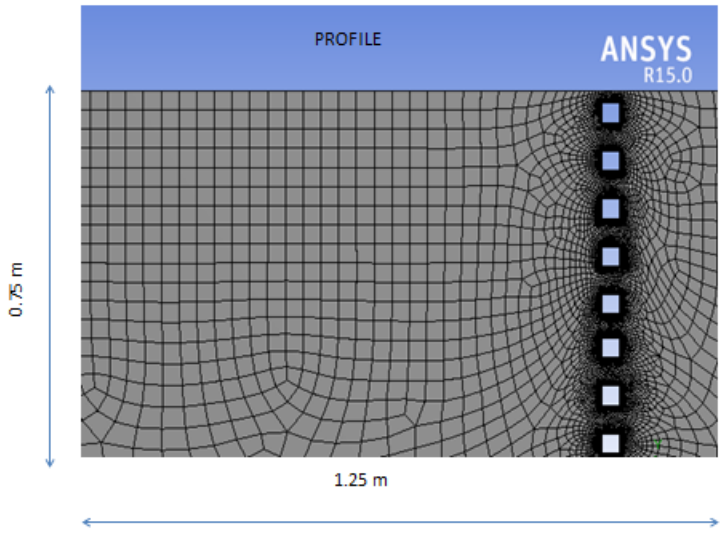

Figure 5: Configuration of the numerical mesh (vertical two-dimensional) near the screens with 60% porosity. The minimum spacing between nodes was 6.0 mm near the screen and increased to a maximum of 3 cm away from the screens.

2.4 Breaking waves

As a wave interacts with other waves at sea its height varies due to the momentum (or energy) exchange with other waves. In general, the wave height increases when the wave receives momentum. But the wave height cannot increase indefinitely, and at some value, the wave becomes unstable and breaks. The breaking manifests through sharp wave crests (thus, there is a "break" in the smooth profile of the wave). If the sharp edge collapses on the front side of the propagating wave, then one obtains a "spilling" breaker. And if the sharp edge curls and renters the water surface forward of the propagating wave, then one obtains a "plunging" breaker. While for regular waves, breaking occurs when the wave height reaches 14% of the wave length, there are no criteria for irregular waves, and thus breaking needs to be generated experimentally. We elected to produce a plunging breakers, as they are more discernible for dispersion effectiveness testing.

There are two major categories for generating breaking waves in wavetanks. The frequency sweep technique (Funke and Mansard 1980) and the dispersive focusing technique(Longuet-Higgins 1973, Rapp and Melville 1990). In the frequency sweep technique, a train of short-period waves (e.g., the period of each wave, T is equal to 1.5 s) is generated followed by a train of long-period waves (e.g., T is equal 3.0 s). As the speed of a wave is proportional to its period, the long-period waves catch up to the short ones, and inject momentum (or energy) into them, which would increase the height of the short waves potentially causing them to break. The dispersive focusing technique requires concentration of multiple components of waves, requiring an advanced programming of the wavemaker, which was not achievable at this juncture. Therefore, the technique for generating breaking wave conditions in the Ohmsett tank was the frequency sweep.

Based on several trials, the following setting of breaking waves was adopted: A train of short-period waves (T = 1.5 s and S = 5 inches=12.7 cm) was first generated for a duration of 6.0 s (i.e., 4 wave cycles), and it was followed by a no-action duration of 18.5 s, and then a train of (relatively) long-period waves (T = 2.0 s and S = 12 inches~30.5 cm) was generated for a duration of 10.0 s (i.e., 5 wave cycles). Then, the wavemaker was stopped for at least 3 minutes.

3.0 RESULTS

3.1 Reflection Experiments

Two wave periods were considered to test the reflection in the wavetank. They were T=2.0 s and T=3.0 s. For each period, the system started from rest, and the wavemaker was run for a duration of 20 minutes, and the water level was recorded using the Ohmsett altimeters (Figure 2). The closest wave gauge (Altimeter 1) to the beach was 50 m from the beach. The distance was intended to be close enough to the beach so that secondary interference in the tank does not mask the effect of reflection. Also, as the wave length for T= 3.0 s is around 12 m (Eq. 2), we decided to place the altimeters four wave-lengths from the beach to minimize the standing wave conditions that are encountered near beaches. Thus, the distance of 50 m seemed reasonable.

Figure 6 provides short time series for T=2.0 s and 3.0 s along with the corresponding reflection coefficient provided by Method 1 (Eq. 7). The R value was approximately 60% and 30% for T=2.0 s and 3.0 s, respectively, as reported in Table 2. This indicates that the beach dissipates the long waves corresponding to 3.0 s better than it dissipates the shorter T=2.0 s waves, which is unusual, as one expects larger reflection from longer waves. Possible explanations include the usage of the first-order theory in Eq. 7, while the system of wave reflection is nonlinear due to, among others, the curved shape of the back wall (i.e., the back wall is not straight but a bit round). Data from other altimeters and for longer durations are reported in the Appendix.

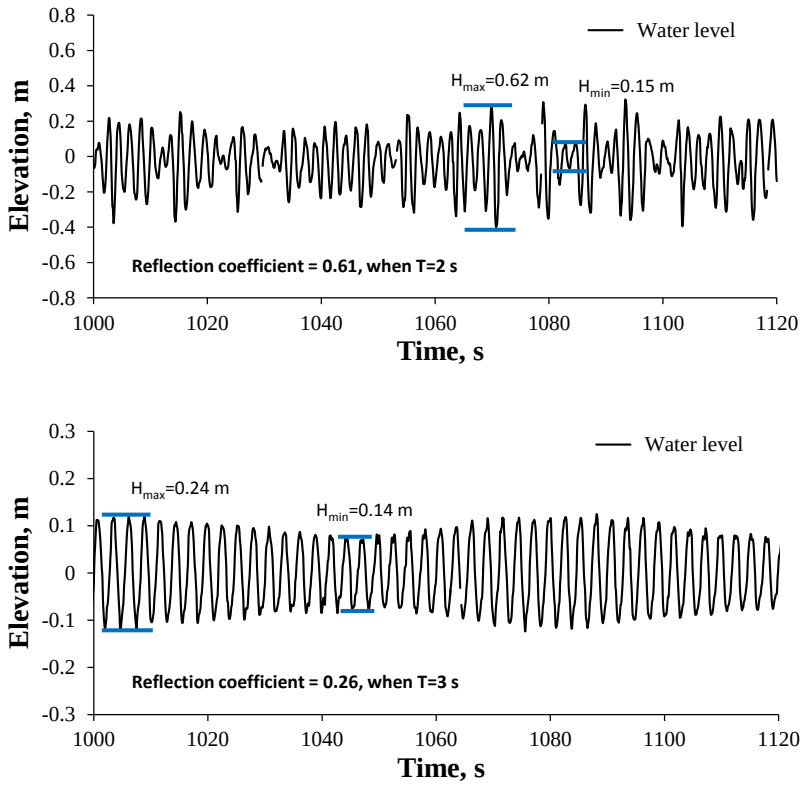

Figure 6: Time series of the water profile obtained at Altimeter 3 (Figure 2). Hmax and Hmin are respectively, the maximum and minimum vertical distances between a crest and the following trough.

When we attempted to use Method 2 on the T=2.0 s waves, we obtained spurious results, which can be due to a variety of non-exclusive factors such as the high reflection coefficient, the presence of secondary harmonics, the occurrence of the altimeters at multiples of half of the wave length, and high nonlinearity of the system, as the waves were very steep. Therefore, the results for T=2.0 s were not reported using Method 2.

Table 2: Measured parameter values and calculated wave reflection coefficient by Method 1 (Eq. 7) and Method 2 (Eq. 6, and Eqs. 8 through 13) for two wave periods, T=2.0 and 3.0 s.

Wave period T=2.0 s		
Parameters	Definition	Measurements
H_{max}	Maximum water level, m	0.62
H_{min}	Maximum water level, m	0.15
Reflection coefficient, R, based on Method 1 (Eq. 7)=		**0.61**
Reflection coefficient, R, based on Method 2 (Eq. 6)=		**NA***
Wave period T=3.0 s		
Parameters	Definition	Measurements
H_{max}	Maximum water level, m	0.24

H_{min}	Maximum water level, m	0.14
Reflection coefficient, R, based on Method 1 (Eq. 7)=		**0.30**
	Method 2 applied to T=3.0 s	
H_1	Average wave height at Altimeter 1, m	0.288
H_2	Average wave height at Altimeter 2, m	0.286
H_3	Average wave height at Altimeter 3, m	0.20
λ_1	Distance between Altimeter 1 and Altimeter 2, m	5
λ_2	Distance between Altimeter 1 and Altimeter 3, m	15
δ_2	Phase angle between Altimeter 1 and Altimeter 2 in radian	2.28
δ_1	Phase angle between Altimeter 1 and Altimeter 3 in radian	0.57
Reflection coefficient, R, based on Method 2a (Eq. 6 and Eqs. 8 through 11)=		**0.28**
Reflection coefficient, R, based on Method 2a (Eq. 6 and Eqs. 8 through 13)=		**0.26**

*: Method 2 did not provide consistent results for T=2.0 s.

For T=3.0 s, Method 2a provided an average wave height of around 0.28 m at both Altimeter1 and Altimeter 2, and 0.20 at Altimeter 3 (see Figure 2a for locations). The reflection coefficient computed by Method2a was equal to 0.28 and was equal to 0.26 by Method 2b, which is remarkably close to the reflection coefficient obtained by Method 1 for T=3.0s, R=0.30 (Table 2).

3.2 Wave Breaking

Using the frequency sweep technique, we report in Figure 7 the results of a plunging breaker. The two wave trains met at around 100 m from the wavemaker where they resulted in a plunging breaker. The breaker was also uniform across the width of the tank, which is in stark contrast to the breakers obtained currently (Figure 3).

Figure 8 reports the variation of the water level before, during, and after the breaker at the three altimeters (note Figure 2b). Before the breaker, the wave height was essentially zero, and the breaker was timed such that the two trains meet at that location, causing a sudden increase in the wave height, followed by water level fluctuations on the order of 0.10m, which decrease within 10 to 20 s, depending on the altimeter. Note that the wave height is the vertical distance between a crest and the trough that follows it. In other words, the breaker height should not be assumed based on the elevation of 0.0, rather relative to other waves. Therefore, the breaker was 0.55 m.

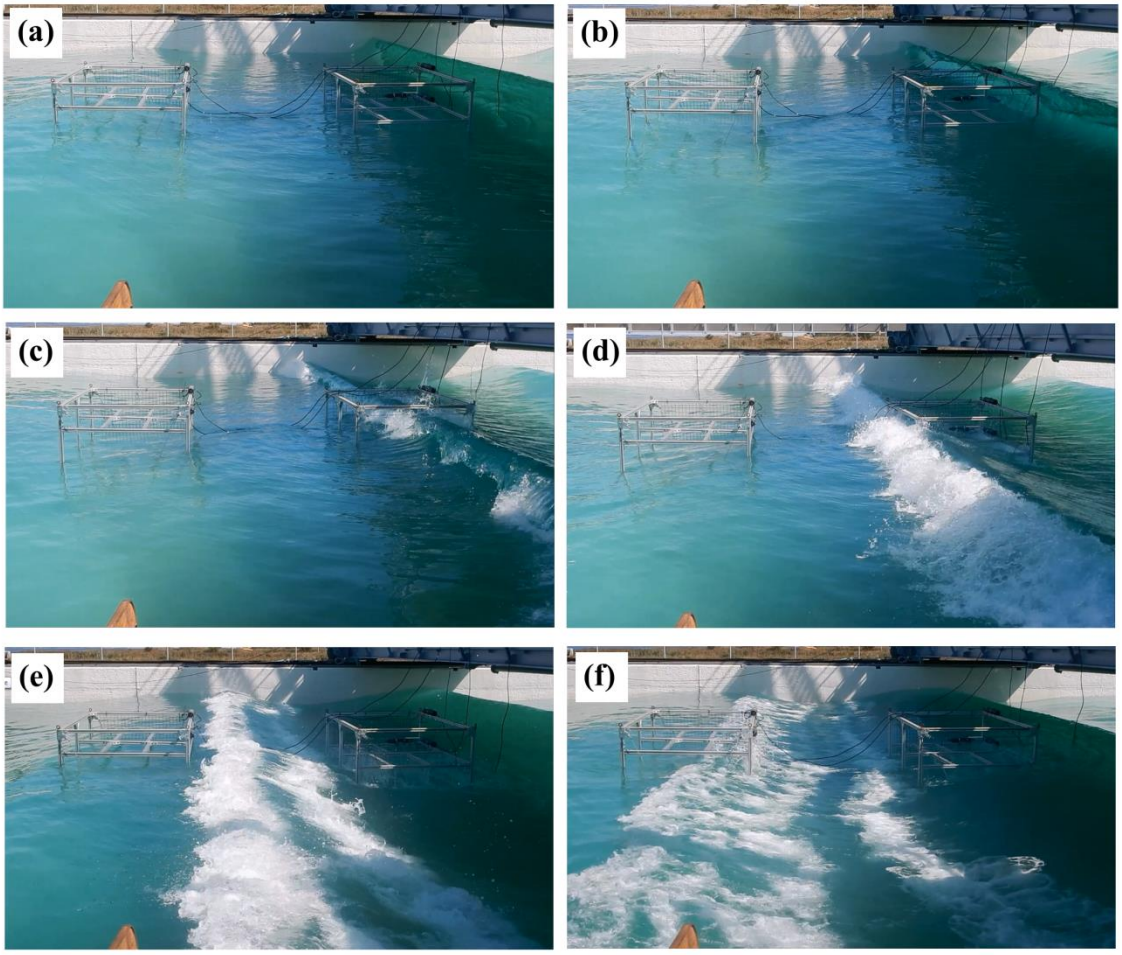

Figure 7: Wave breaking using the Frequency Sweep method captured using camera on the side of the tank. Note how the breaker across the whole tank and is very violent.

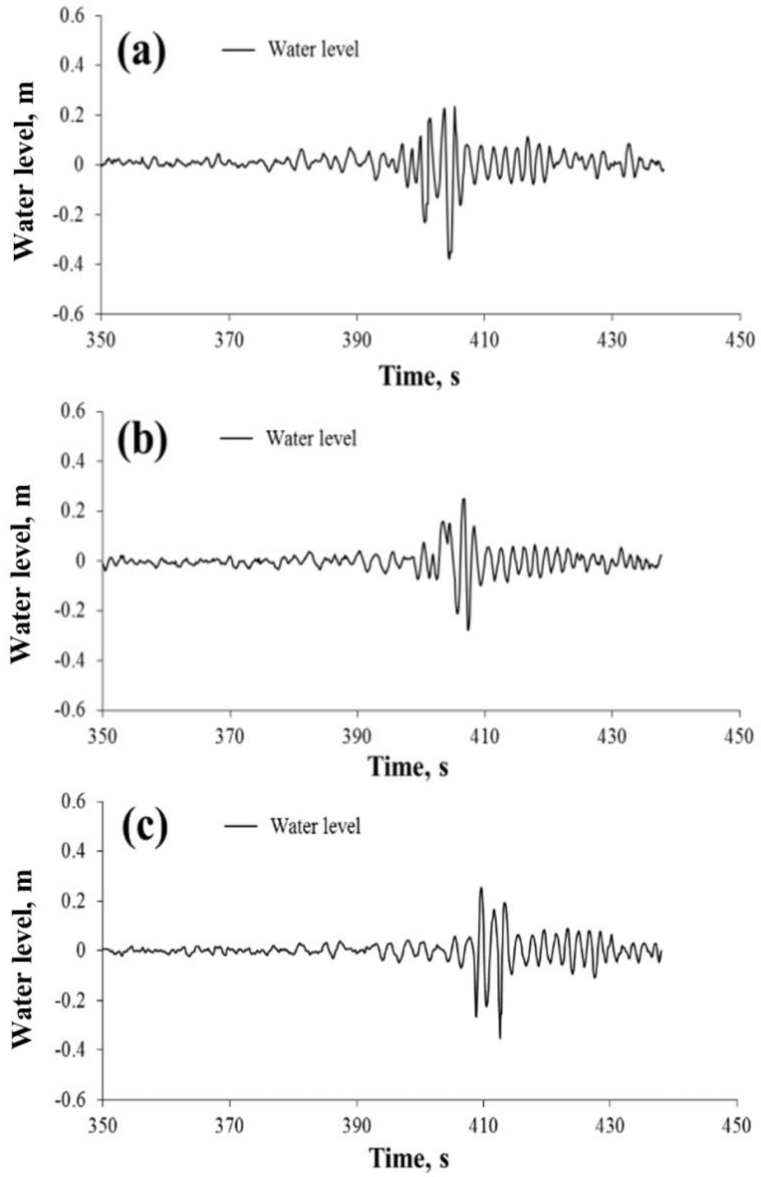

Figure 8: Temporal variation of the water level during the breaking experiment measured at (a) altimeter 1, (b) altimeter 2, and (c) altimeter 3 for wave breaking tests. Results are shown as difference with the Mean Water Level (MWL), which is the average water level in the tank. The altimeter locations are reported in Figure 2b.

Figure 9 reports the time series of the velocity obtained from the ADV, which was 1.2 m above the bottom of the tank, thus 1.2 m below the Mean Water Level (MWL) of 2.4 m. One notes a rapid increase in the velocity due to the breaker, especially in the longitudinal and vertical directions. This indicates that the plunging breaker could entrain surface oil deep into the tank and not simply disperse it near the water surface. In addition, the lateral (horizontal across the tank) velocity (i.e., in the y direction) was comparatively small suggesting that the breaker was uniform. Note that the increase in the lateral velocity is expected and is due to increased turbulence.

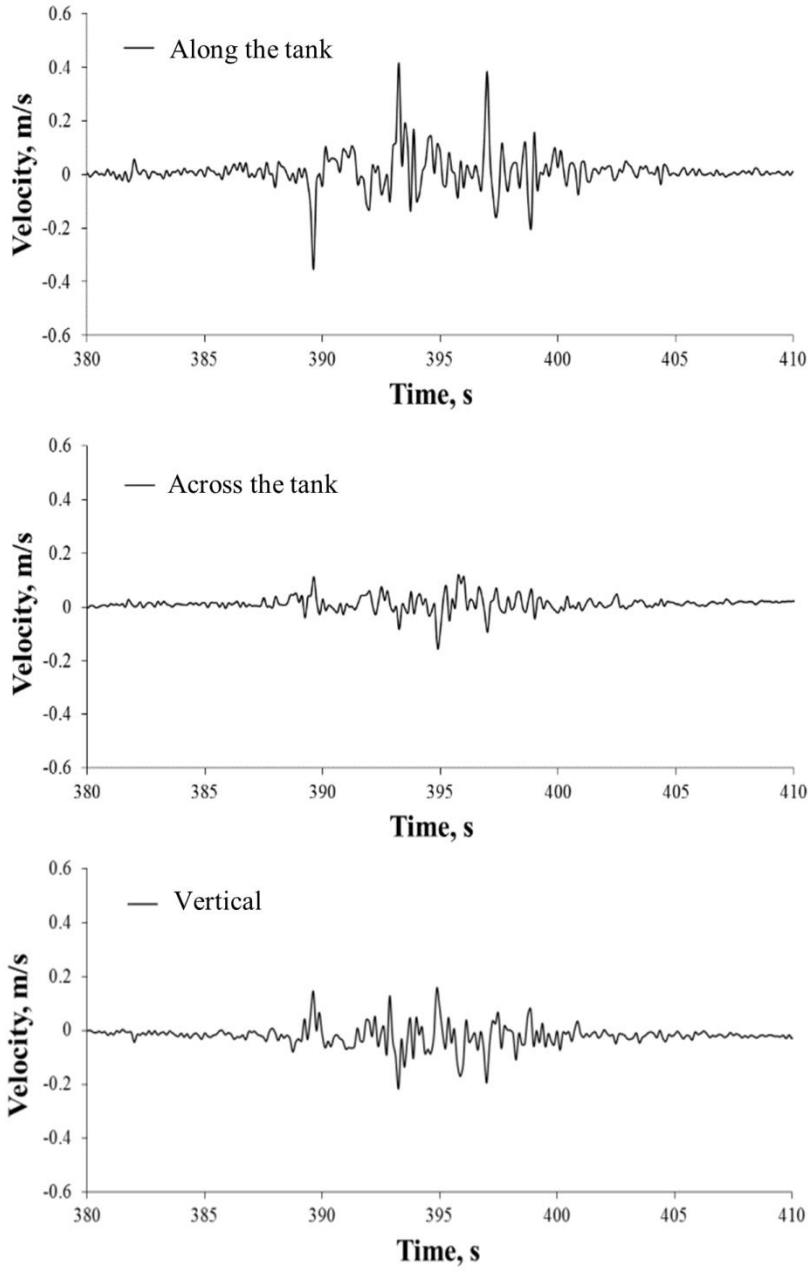

Figure 9: Measured temporal variation of the velocity components during the breaking event in three directions at 1.2 m deep (from the Mean Water Level). (a) horizontal along the tank (i.e., x direction), (b) horizontal across the tank (i.e., y direction), and (c) vertical (i.e., *z* direction).

3.3 Design of system to reduce wave reflection

This task was conducted numerically as discussed in Section 2.3. The wave period was assumed to be 2.0 s, which gives a wave length of approximately 6.3 m (Eq. 2). The wave height (vertical distance between crest and trough) prior to breaking was 0.6 m, which is close to the commonly

used value in the Ohmsett tank for T=2.0 s (Table 1). It is less than the theoretical maximum of 0.88 m for the 2.0 seconds wave, which is around 14% of the wave length (Eq. 5).

Figures 10, 11, and 12 show the water surface level as the wave train (corresponding to 13 periods of simulation times) traveled through the screens at time snap-shots of 8 s, 16 s, and 26 s, respectively. Time zero was when the first wave impacted the first screen. The water profile showed similar trends for both submergence cases when the waves passed through the screens.

At time t=8s (Figure 10), the water profile did not change much from the general wave shape when the waves passed through the higher porosity screens (between 6 and 12m). However, there was a severe change in the second set of screens (x between 0 to 6 m), and the wave height there decreased significantly from 0.60 m to 0.10 m at the wall, and this occurred for both cases of submergence.

At later time, t=16 s and 26 s (Figures 11 and 12), one notes a gradual variation of the volume fractions with elevation between the screens. This suggests the formation of "foaming" conditions between the screens, which would dissipate the wave energy. The fact that the downstream water level is affected by the reflected waves indicates that both of the systems with fully and partially submerged screens suffer from reflection although both successfully dissipate the wave energy.

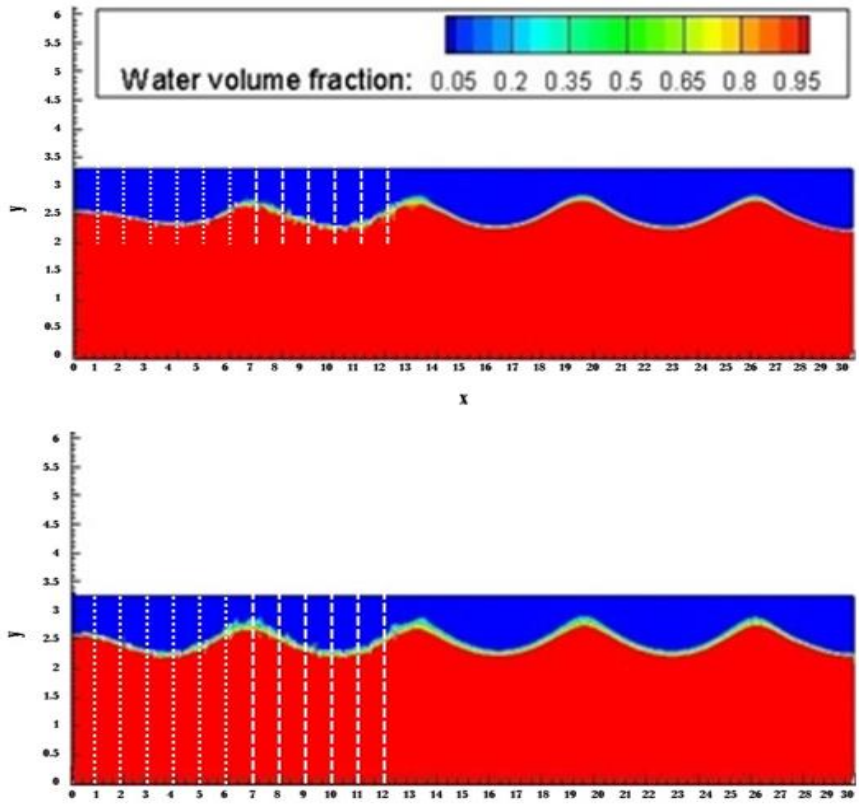

Figure 10: Water profile as provided by the volume fraction at time 8 s after the first impact. The top panel corresponds to partially submerged screens and the bottom panel corresponds to fully submerged screens.

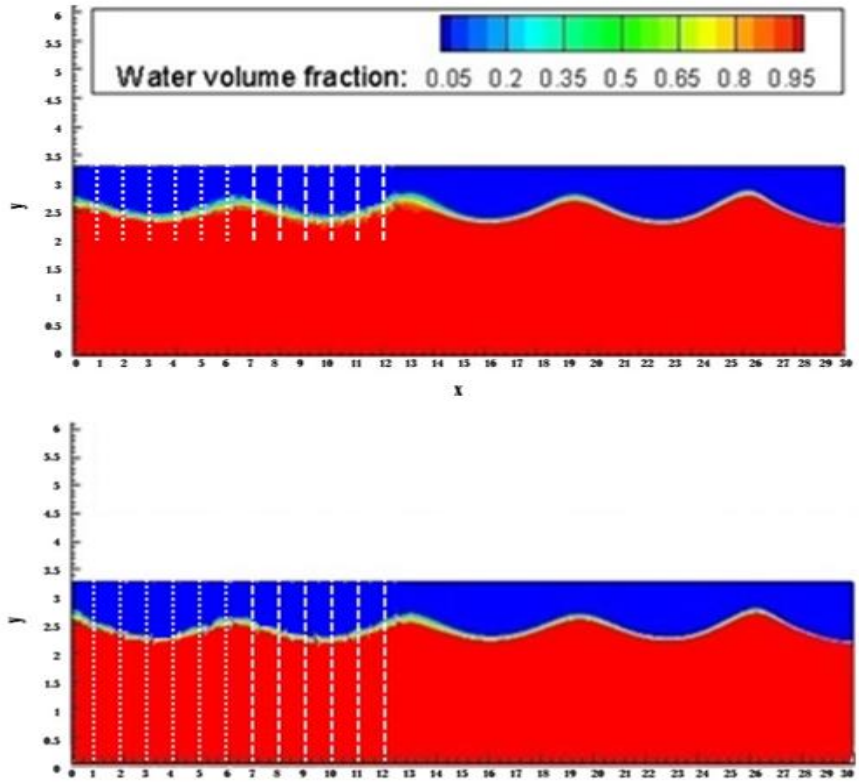

Figure 11: Water profile as provided by the volume fraction at time 16 s after the first impact. The top panel corresponds to partially submerged screens and the bottom panel corresponds to fully submerged screens

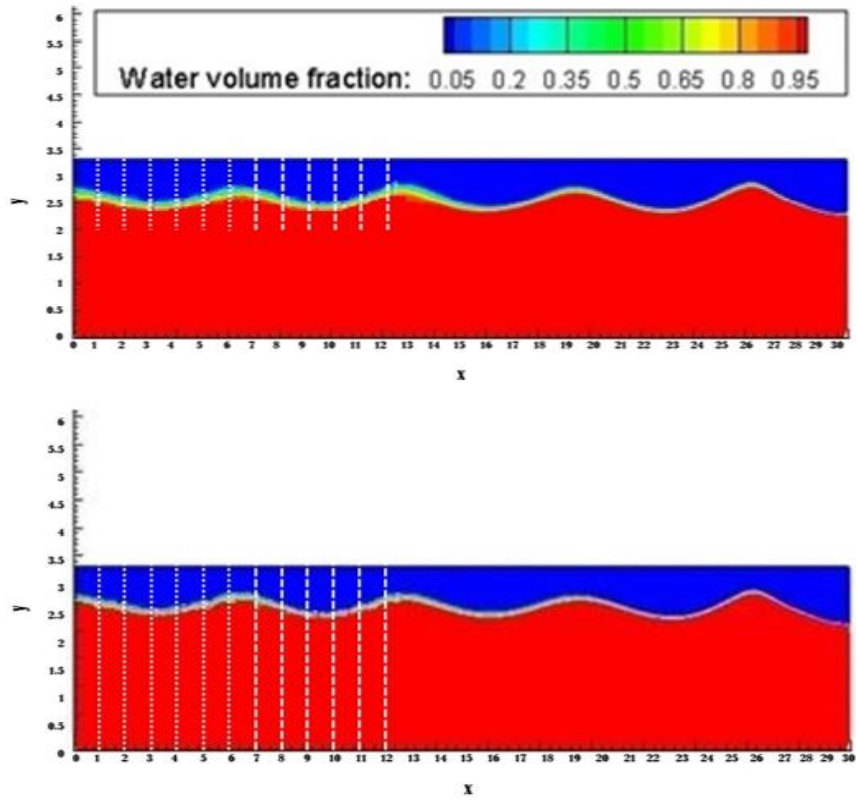

Figure 12: Water profile as provided by the volume fraction at time 26 s after the first impact. The top panel corresponds to partially submerged screens and the bottom panel corresponds to fully submerged screens.

Figure 13 presents the computed time series of reflection coefficient for both cases. The reflection induced by the fully submerged screens is smaller than that of the scenario with partially submerged screens. This is due to the fact that the space below the partially submerged screens allows the lower part of the wave train to pass without being dissipated, and thus the train gets reflected back after impinging on the back wall (at x=0.0 m). The values of the reflection coefficient however, are less than 10% suggesting that the partial screen configuration is acceptable as a preliminary design.

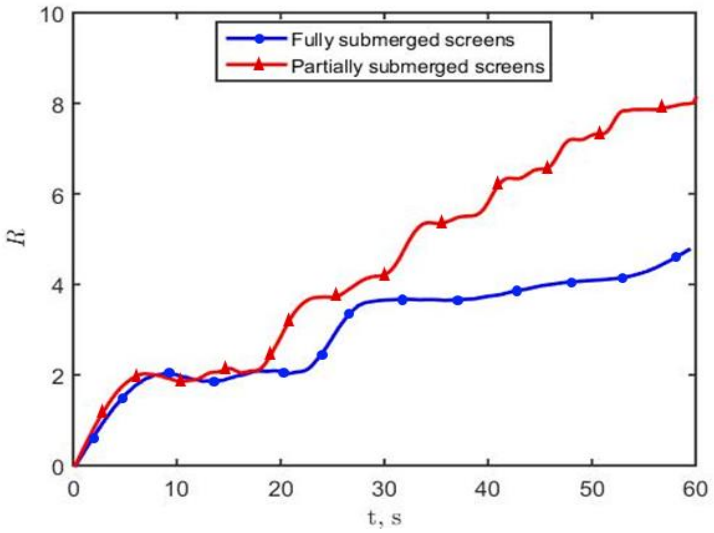

Figure 13: Time evolution of the calculated reflection coefficient R as % using Method 2a (Eqs. 6, and 8-11) for the simulation with partially and fully submerged screens. The start time 0 s corresponds to the time of the first wave impacting the first screen (see Figure 4).

Figures 14-16 show velocity magnitude contours for both screen submergence scenarios, and at time snap shots varying between 8 to 26 seconds after the time when the first wave impacted the first screen (time 0). We first focus on the velocity magnitude in the area below the screens in the scenario with partially submerged screens (between 0 and 12 m and y between 0 to 1.5 m). Comparing the velocity magnitudes of the partially submerged screens (top panels of Figures 14-16) to those of the scenario with fully submerging screens (bottom panels of Figures 14-16), one realizes that the maximum velocity values are slightly higher for the scenario with partially submerged screens. This, among others, explains the slightly larger reflection coefficient of the scenario with partially submerged screens.

Upstream of the screen area (x between 12 m and 20 m), the maximum value of velocity magnitude decreases with time for both screen submergence cases, which is a manifestation of reflection. The decrease in velocity for the fully submerged screens (bottom panels of Figures 14-16) is smaller than that of the case with partially submerged screens (top panels of Figures 14-16), which is consistent with the finding in Figure 13 that full submergence of the screens produced a smaller reflection.

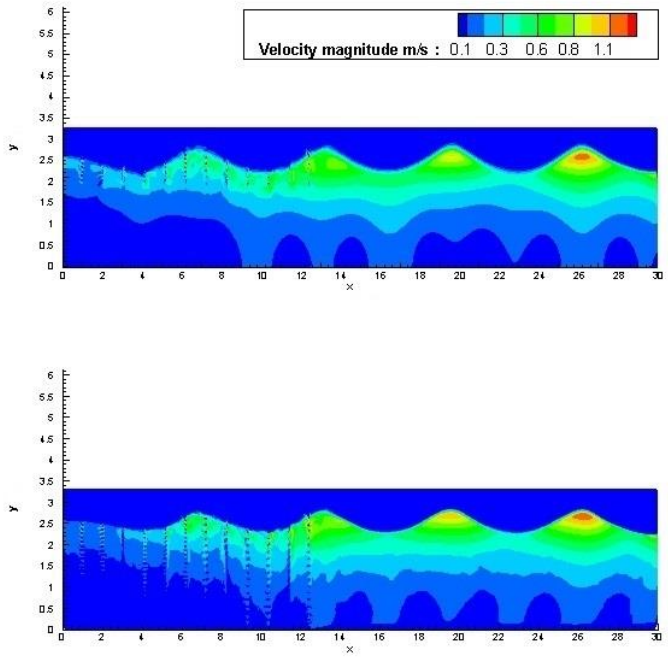

Figure 14: Velocity magnitude at time 8s after the first impact. The top panel corresponds to partially submerged screens and the bottom panel corresponds to fully submerged screens.

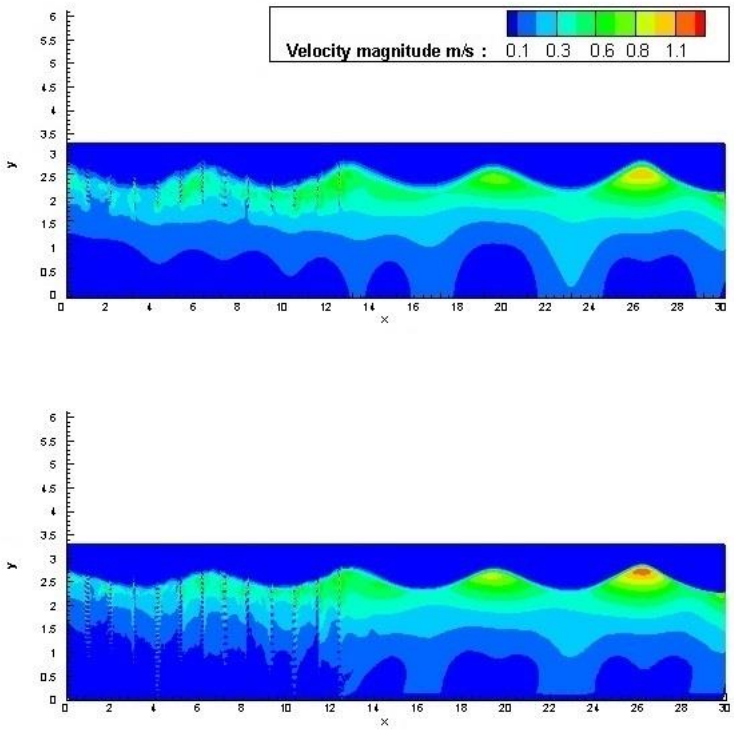

Figure 15: Velocity magnitude at time 16 s after the first impact. The top panel corresponds to partially submerged screens and, the bottom panel corresponds to fully submerged screens.

.

.

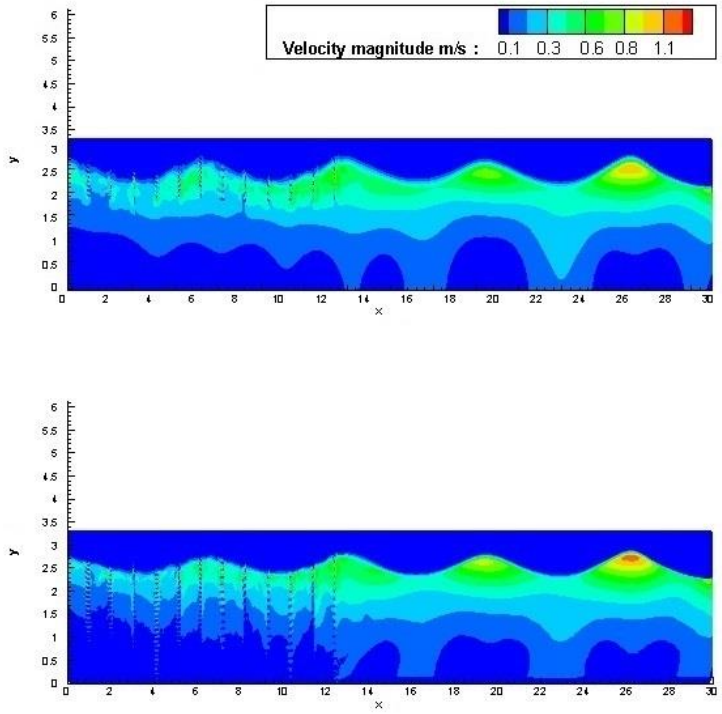

Figure 16: Velocity magnitude at time 26 s after the first impact. The top panel corresponds to partially submerged screens and, the bottom panel corresponds to fully submerged screens.

The dynamic pressure represents the increase in water pressure due to an increase in the water momentum. It is different from the static pressure, which depends on the water height, and tends to cancel out when water is on both sides of an object, such as the screens. Figure 17 - 19 show dynamic pressure contours for both submergence scenarios of the screens, and at time snap shots varying between 8 to 26 seconds after the time when the first wave impacted the first screen (time 0). The dynamic pressure is higher for the scenario with partially submerged screens (top panels of Figures 17-19) when compared to that of the scenario with fully submerged screens (bottom panel of Figures). In the near wall region (x between 0 and 6 m) the value of the dynamic pressure is low for both cases, which suggests that the screens dissipated wave energy successfully. But in all cases, the increase in the dynamic pressure is relatively small (less than one kPA, which is around 0.10 m of water), and it is expected that the structures holding the steel screens in place would be able to sustain such a pressure.

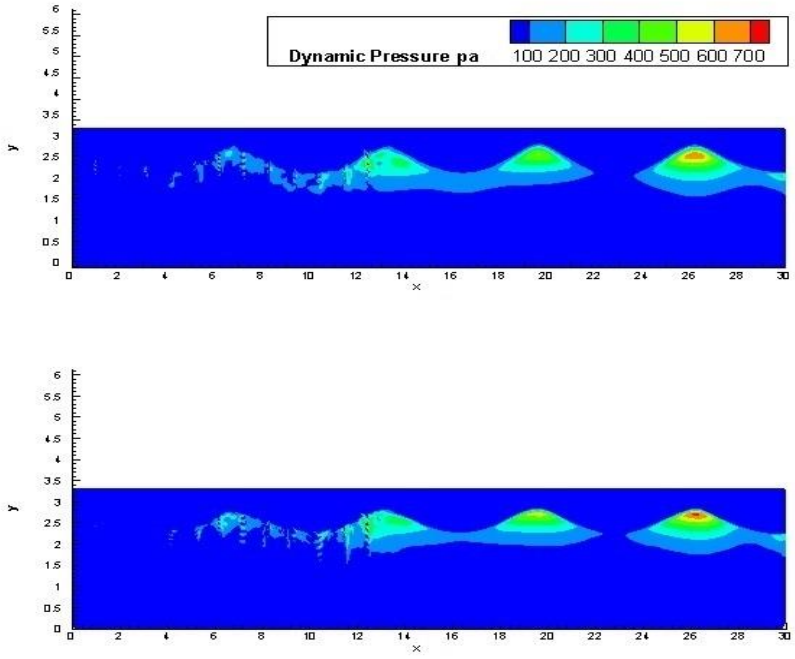

Figure 17: Dynamic pressure at time 8 s after the first impact. The top panel corresponds to partially submerged screens and, the bottom panel corresponds to fully submerged screens. The quantity 700 pa is approximately equal to 0.07 m (less than 3 inches of water), which is approximately equal to 0.1 psi.

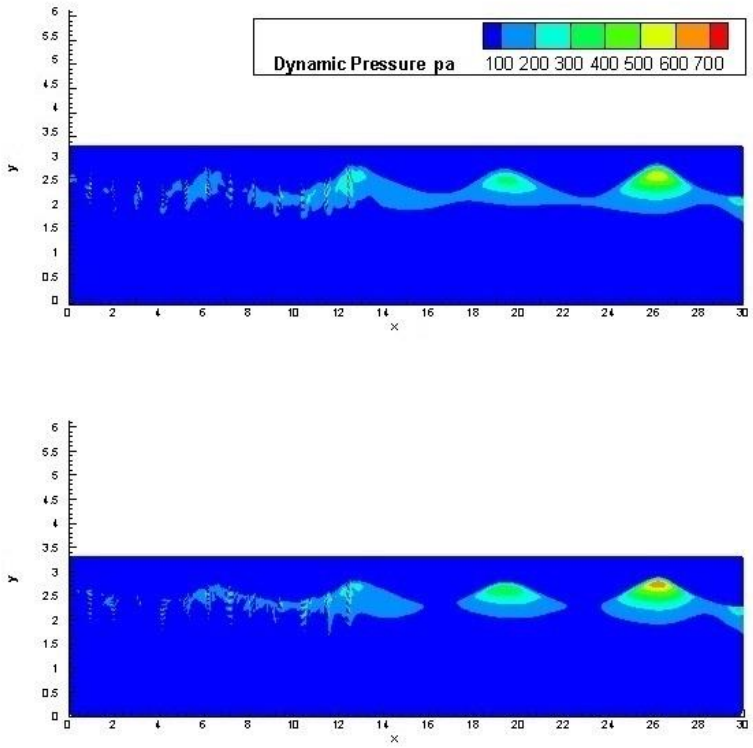

Figure 18: Dynamic pressure at time 16 s after the first impact. The top panel corresponds to partially submerged screens and, the bottom panel corresponds to fully submerged screens. The quantity 700 pa is approximately equal to 0.07 m (less than 3 inches of water), which is approximately 0.1 psi.

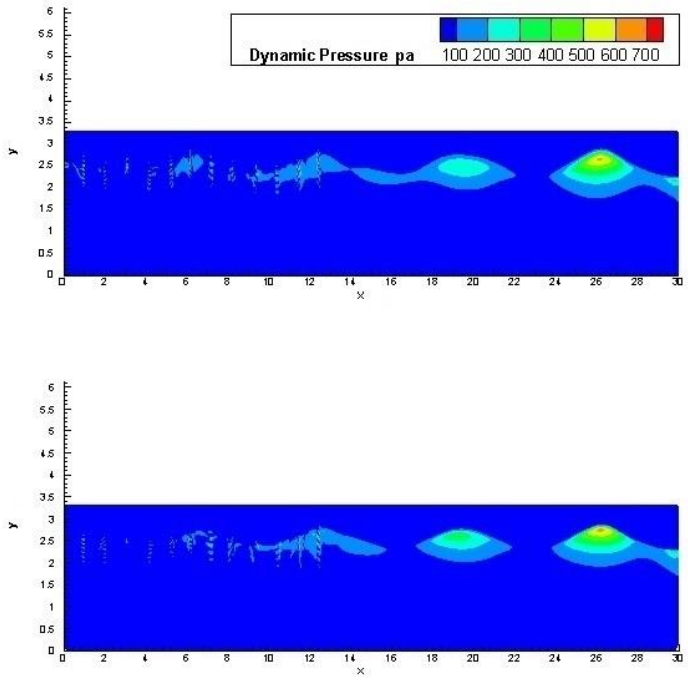

Figure 19: Dynamic pressure at time 26 s after the first impact. The top panel corresponds to partially submerged screens and, the bottom panel corresponds to fully submerged screens. The quantity 700 pa is approximately equal to 0.07 m (less than 3 inches of water), which is approximately equal to 0.1 psi.

Section 4.0 Summary and Discussion

The goal of this project was to address three objectives related to the hydrodynamics in the Ohmsett wavetank. They are:

a) Evaluate the reflection in the wavetank based wave properties that are commonly generated in the Ohmsett tank.
b) Generate breaking wave conditions in the Ohmsett tank that are reproducible and their mixing energy can be quantified.
c) Design, using Computational Fluid Dynamics, a system to dissipate the wave energy and thus reduce wave reflection.

Regarding the first objective (Objective "a" above), one needs to compute the reflection coefficient, which was computed herein using two standard methods based on the time series of water level data computed at Altimeter 1 (Figure 3). In Method 1, one uses the formula:

$$R = \frac{H_{\max} - H_{\min}}{H_{\max} + H_{\min}} \qquad (7)$$

Where H_{max} and H_{min} are the maximum and minimum wave heights in a time series (see Figure 6). This is an empirical method, and it provided R~30% and 60% for T=3.0 s and T=2.0s ,

respectively. Method 2 is more elaborate, and has two variants, each provided R~30% for T=3.0 s (Table 2). Method 2 provided inconsistent results for T=2.0 s, and thus was not used for that case. It was expected that the reflection coefficient would be larger for longer waves. However, the large value for T=2.0 s could be to two non-exclusive factors:

1) Wave steepness, defined as:

$$St = \frac{H}{L} \tag{11}$$

For T=2.0 s, we had (H=0.6 m and L=6.0 m) resulting in St(2.0 s)= 10% while for T=3.0s, we had (H=0.3 m and L=13.0 m) resulting in St(3.0 s)=2.2 %. Therefore, the T=2.0 s waves were close to their maximum value inducing a large degree of nonlinearity. As the current methods for evaluating reflection rely on the linear theory, it is likely that there is a large uncertainty associated with the results.

2) Imperfection in the Ohmsett tank.

We have always assumed that the flow in the Ohmsett tank is two-dimensional (along the long side of the tank and vertical). However, due to the large width of the tank, imperfections in the wavemaker, and the fact that the back wall of the tank is curved (not straight), three-dimensional hydraulics is present in the tank. This can be deduced from Figure 3, where the breaker is not across the tank. Had the flow been two-dimensional (vertical and along the long side of the tank) then the breaker would be across the tank.

For Objective "b" (breaking wave conditions), we used the frequency sweep method and generated reproducible breakers. The breaker was generated as follows: A train of short-period waves (T = 1.5 s and *Stroke* = 5 inches=12.7 cm) was first generated for a duration of 6.0 s (i.e., 4 wave cycles). It was followed by a no-action duration of 18.5 s, and then a train of T = 2.0 s (and *Sroke* = 12 inches~30.5 cm) were generated for a duration of 10.0 s (i.e., 5 wave cycles). The two wave trains met at around 100 m from the wavemaker, where they resulted in a plunging breaker, as shown in Figure 7. The breaker was also uniform across the width of the tank, which is in stark contrast to the breakers obtained currently (Figure 3).

Due to the existing reflection in the tank, we could only generate breakers every two minutes, as we had to let wave reflection dissipate before we started the short-wave train, otherwise, the breaker is not as obvious (or "clean"). Thus, with the current "beach" of the Ohmsett tank, one could not generate waves separated by less than two minutes, but by any duration larger than two-minutes.

A method known as dispersive focusing was used by our group in the past in other tanks (Botrus, Boufadel et al. 2008), and is able to generate more violent breakers. Also, it allows for a larger flexibility in terms of the location and time of the breaker. But the method requires programing the wavemaker by the electronics company Next Step Controls that is managing the electronics of the Ohmsett wavetank. However, this could not take place within the duration of the project.

For Objective “c” (screens to minimize reflection), we considered a series of twelve screens spaced by 1.0 m (resulting in 12 m from the back wall to the first screen facing the wavemaker). The first six screens (facing the wavemaker) had a porosity of 75% while the second set of six screens had a porosity of approximately 60%. We also considered two situations: One where the screens were partially submerged, by 0.4 m from the Mean Water Level (see Figure 4) and another where they were completely submerged.

The reflection coefficient based on Eq. 6 and 8-10 is reported in Figure 13, and it was smaller than 10% and 5% for the partially and completely submerged screens, respectively. Considering that the current reflection for the 3.0 s waves is around 30%, the screens would reduce reflection in the tank considerably. In addition, the reflection coefficient from these screens was computed at x=18 m (i.e., 6.0 m from the first encountered screen by the waves, Figure 4), and the reflected waves and subsequently the reflection decrease going toward the wavemaker. Therefore, the large length of the tank would induce further dissipation of the reflected waves by the time they reach 100 m into the tank, where experiments are typically conducted. However, it was computationally too expensive to model the hydrodynamics in the whole Ohmsett tank at this juncture.

The dynamic pressure on the screens was found to be less than 1.0 kPA (i.e., less than 0.10 m of water), a relatively small value that would be easily withstood by steel structures holding the screens.

Acknowledgment

We benefited tremendously from collaboration with the Ohmsett personnel during this project. We thank them for their technical support and professionalism. We are in particular indebted to Mr. Alan Guarino, who was critical in guiding the NJIT staff to generate the breaker.

REFERENCES

Botrus, D., et al. (2008). Wave tank to simulate the movement of oil under breaking waves. Proceedings of the 31st AMOP Technical Seminar on Environmental Contamination and Response.

Boufadel, M. C., et al. (2008). Theoretical foundation for predicting dispersion effectiveness due to waves. International Oil Spill Conference, American Petroleum Institute.

Dean, R. G. and R. A. Dalrymple (1991). Water Wave Mechanics for Engineers and Scientists. New Jersey, Prentice-Hall Inc., 1984. Reprinted Singapore: World Scientific Publishing Co.

Funke, E. R. and E. P. Mansard (1980). On the synthesis of realistic sea states. Proceedings of the 17th coastal engineering conference, ASCE.

Goda, Y. and A. T. Ippen (1963). Theoretical and experimental investigation of wave energy dissipators composed of wire mesh screens, MIT Hydrodynamics Lab**:** 66.

Hasselmann, K., et al. (1973). "Measurements of wind-wave growth and swell decay during the Joint North Sea Wave Project (JONSWAP)."

Hughes, S. A. (2005). Physical models and laboratory techniques in coastal engineering, Advanced Series on Ocean Engineering

Isaacson, M. (1991). "Measurement of regular wave reflection." Journal of Waterway, Port, Coastal and Ocean Engineering. ASCE **117**(6): 553-569.

Keulegan, G. H. (1972). Wave damping effects of fibrous screens. U. A. E. W. e. station. Vicksburg, Mississippi.

Le Mehaute, B. (1972). "Progressive wave absorber." Journal of Hydraulic Research **10**(2): 153-169.

Longuet-Higgins, M. S. (1973). Breaking waves in deep or shallow water. Proceedings of the 10th

Conference on Naval Hydrodynamics, Massachusetts Institute of Technology.

Ouellet, Y. and I. Datta (1986). "A survey of wave absorbers." Journal of Hydraulic Research **24**(4): 265-280.

Rapp, R. and W. Melville (1990). "Laboratory measurements of deep-water breaking waves." Philosophical Transactions of the Royal Society of London. Series A, Mathematical and Physical Sciences: 735-800.

Wickley-Olsen, E., et al. (2007). Regular and Breaking Waves in Wave Tank for Dispersion Effectiveness Testing. Proceedings of the Arctic and Marine Oil Spill, Edmonton Alberta, Canada.

Wickley-Olsen, E., et al. (2008). Regular and Breaking Waves in Wave Tank for Dispersion Effectiveness Testing. Proceedings of the International Oil Spill Conference, Savannah Georgia, USA.

Appendix

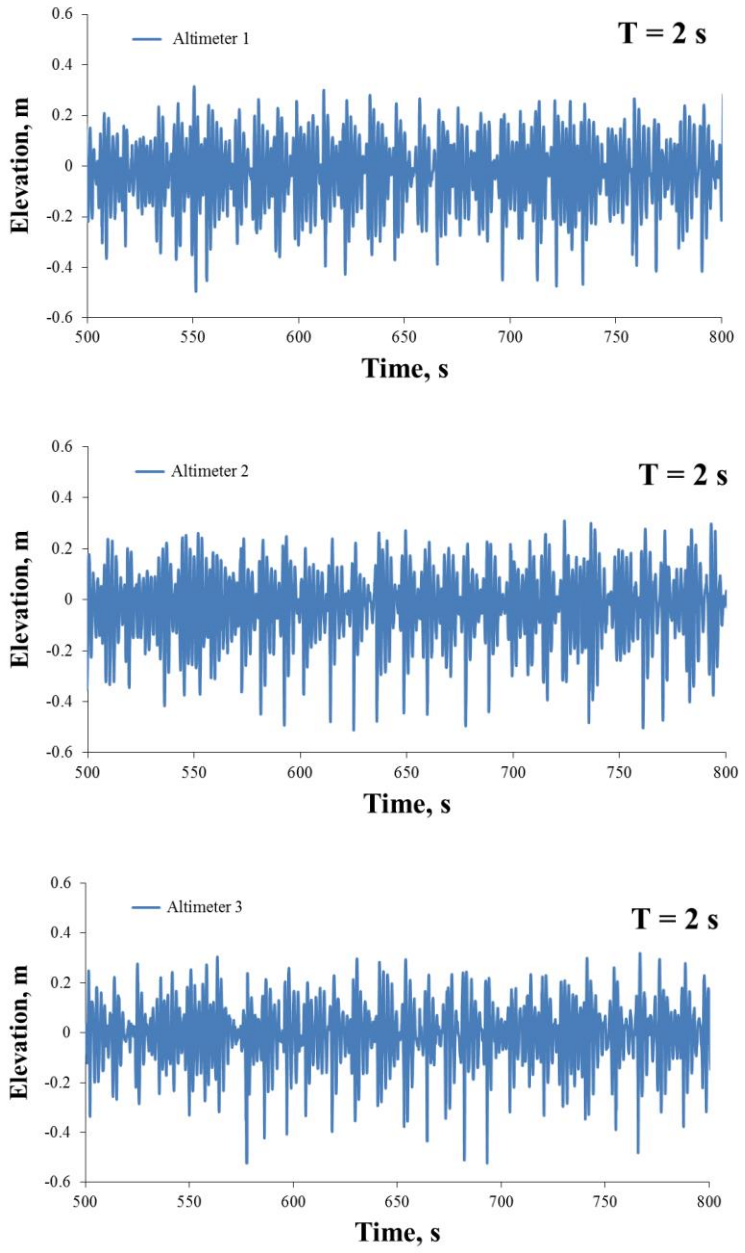

Figure A1: Time series of the three altimeters during the reflection experiments for T=2.0 s. Note how the water level varies wildly with time indicating a highly nonlinear system, and high reflection, as small reflection would result in essentially a smooth, constant wave height profiles.

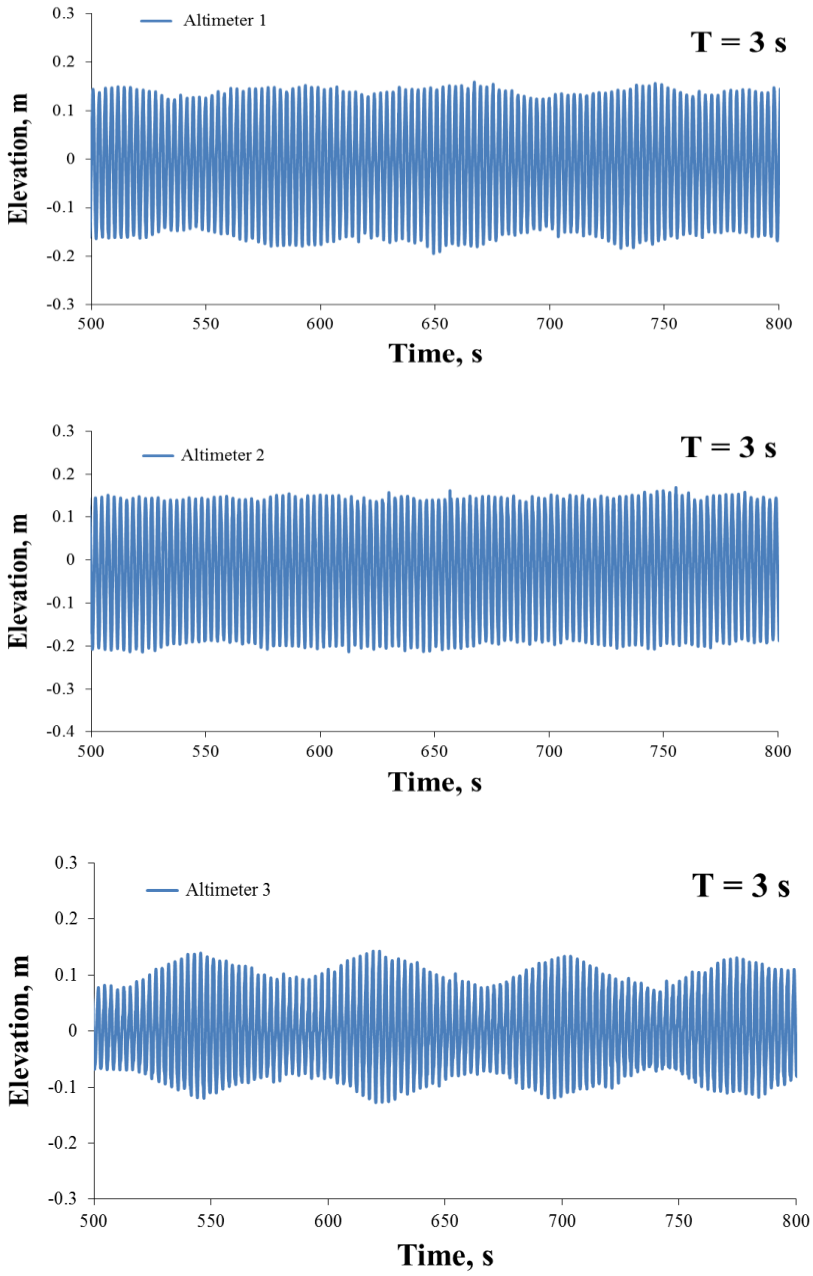

Figure A2: Time series of water level during the wave reflection experiments for T=3.0 s. Note how the wave height varies over time, indicating a large contribution of the reflection.

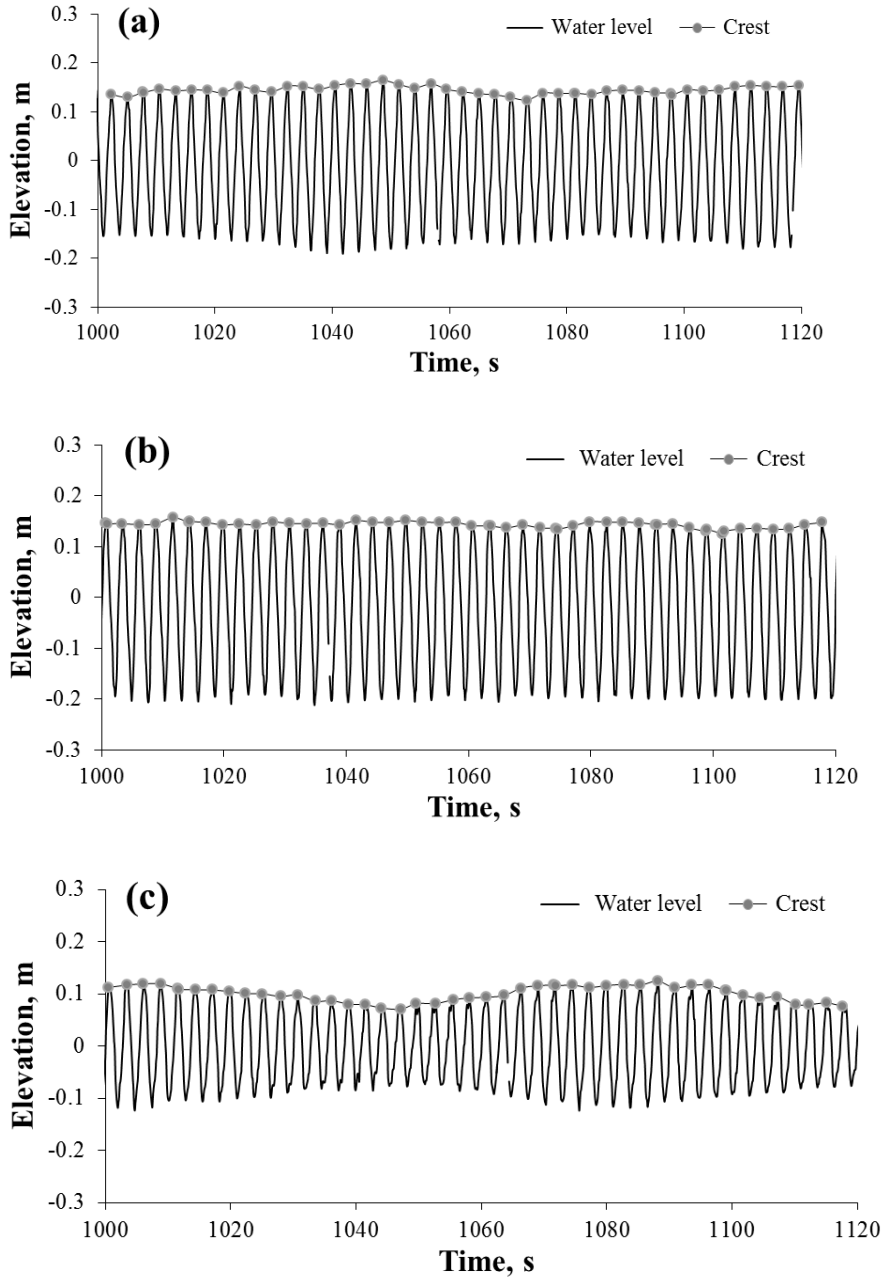

Figure A3: Temporal variation of wave-induced water level measured at (a) altimeter 1, (b) altimeter 2, and (c) altimeter 3 for wave reflection tests. The altimeter locations are shown in Figure 2a.

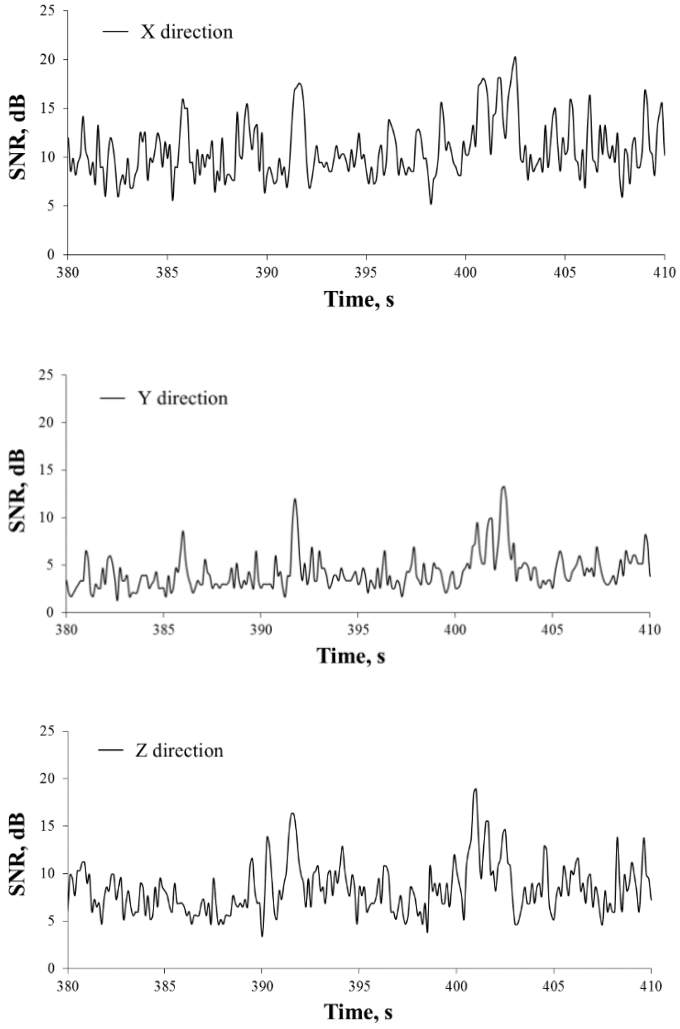

Figure A4: Temporal variation of the SNR (Signal-to-Noise Ratio) (a) along the tank (i.e., x direction), (b) horizontal across the tank (i.e., y direction), and (c) perpendicular to the tank (i.e., z direction).

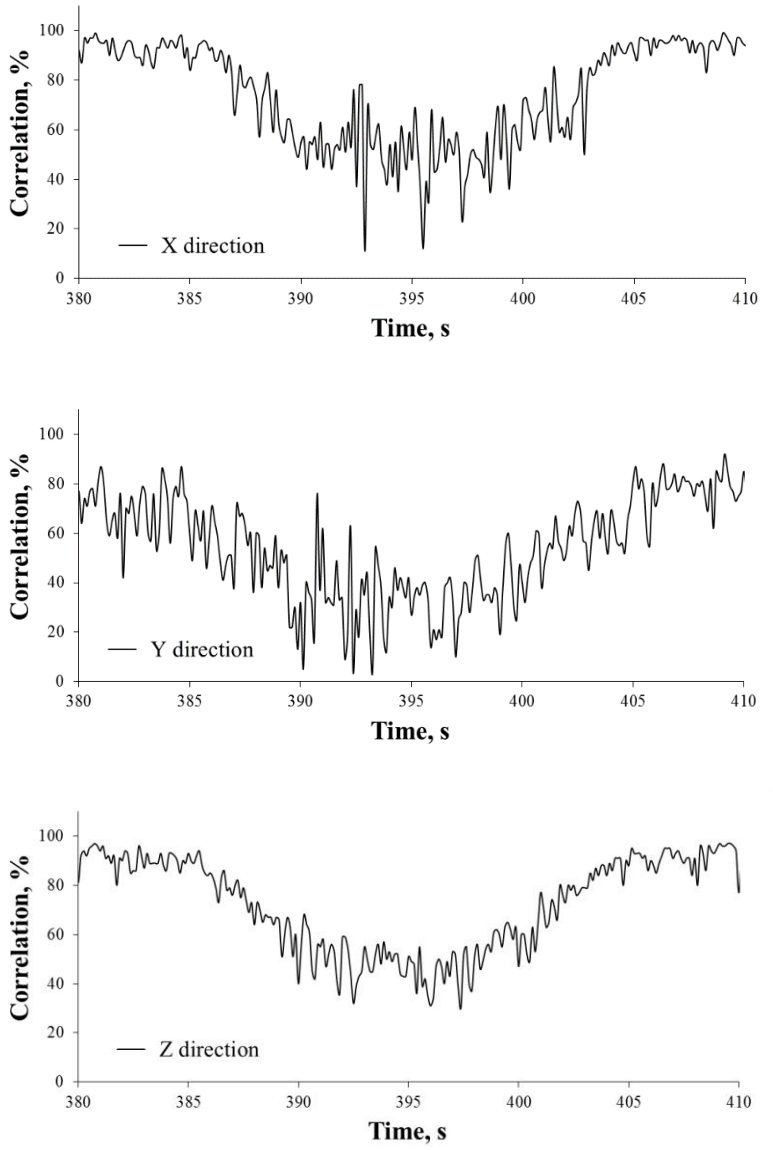

Figure A5: Temporal variation of the Correlation of ADV measurements (a) along the tank (i.e., x direction), (b) horizontal across the tank (i.e., y direction), and (c) perpendicular to the tank (i.e., z direction).

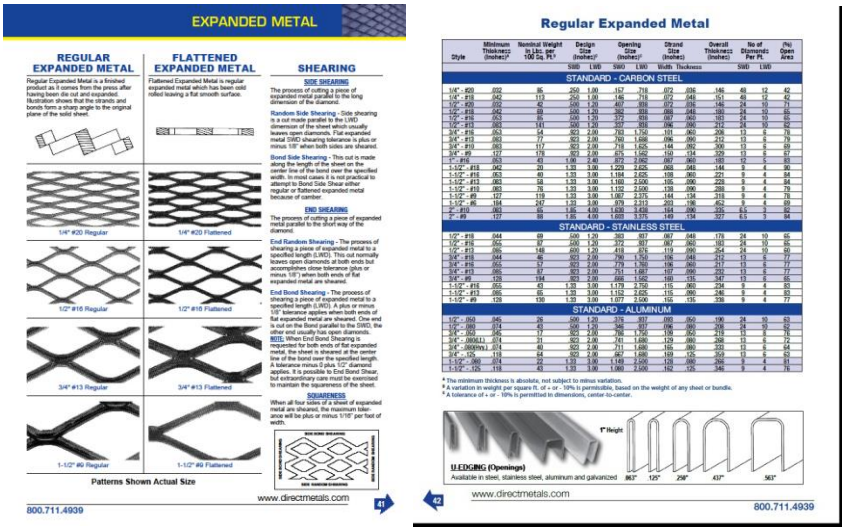

Figure A6: Expanded steel that could be used as material for the screens to dissipate wave energy. No endorsement of the manufacturer is implied.